RESEARCH PAPER

PCCP
www.rsc.org/pccp

Studying reaction kinetics by simultaneous FRET and cross-correlation analysis in a miniaturized continuous flow reactor

Petra S. Dittrich,[a] Barbara Müller[a] and Petra Schwille[ab]

[a] *Experimental Biophysics Group, Max-Planck-Institute for Biophysical Chemistry, Am Fassberg 11 D-37077 Göttingen, Germany*
[b] *Institute for Biophysics/BIOTEC, TU Dresden, Tatzberg 47-51 D-01307 Dresden, Germany*

Received 11th May 2004, Accepted 2nd July 2004
First published as an Advance Article on the web 14th July 2004

In this study we present a refined optical detection technique for investigation of fast reactions based on confocal fluorescence spectroscopy in a miniaturized continuous flow (μCF) reactor. The special setup allows for simultaneous observation of the reaction on the basis of fluorescent resonance energy transfer (FRET) as an indicator of the reaction progress. Determination of the flow velocity *via* spatial fluorescence cross-correlation enables the conversion of spatial information, *i.e.* the position of the detection point, into the respective temporal information. To overcome the disadvantage of conventional continuous flow reactors of high sample consumption, we used a microfluidic chip allowing an economical expenditure of sample solution at low concentration, while the silicon/glass chip is perfectly adaptable to the confocal setup. Inside these channels, rapid, diffusion-based mixing under laminar flow conditions is performed at the crossing of three channels by squeezing the solutions into thin layers. Using this μCF device, we investigated the irreversible cleavage reaction of a double stranded DNA oligomer by the enzyme exonuclease III. The complementary DNA strands are stained with TAMRA and Cy 5 dye molecules, respectively, undergoing an energy transfer if both strands are annealed. The reduction of the Cy 5 fluorescence directly corresponds to the progress of the cleavage reaction.

Introduction

Time-resolved kinetic studies of chemical and biochemical processes provide essential information for a detailed understanding of molecular interaction and reaction mechanisms. However, many of these reactions occur on very short time scales that render an appropriate time resolution particularly hard for conventional techniques of data collection. Thus, a wide variety of techniques have been proposed in the past and developed for the initiating and probing of fast reactions in the time scale of microseconds and below, such as relaxation techniques for reversible reactions induced by temperature or pressure jumps,[1,2] or flash photolysis for light-induced reactions.[3]

Many biological reactions, *e.g.* enzymatic catalysis, are induced by mixing and collision of two (or more) reactants. For the observation of fluid-based reactions in general, continuous and stopped flow methods were introduced quite early on [4] and since then have been constantly improved with respect to temporal resolution from a few seconds down to the submicrosecond regime.[5,6] The beauty of the continuous flow kinetics is the concept of transforming the temporal information into a spatial one, supporting the simultaneous observation of a system at different time points by spatially resolved detection.

In spite of their conceptual elegance, continuous flow experiments usually suffer from the practical drawback that large amounts of sample solution are consumed during the experiment, which has in the past limited their applications. However, in the age of micro- and nanotechnology, these rather old-fashioned concepts have gained a wholly new relevance. By a consequent downscaling of the channel dimensions to micrometer dimensions, the reaction volume can be tremendously decreased to the order of a few μL. Additionally, using a proper channel design, there is basically no dead volume (defined as the volume between the point where the reaction is initiated, and the first observation point).

There is one significant difference to the standard applications, though:[7] On such small scales, the flow is strictly laminar. The Reynolds (*Re*)-number—determined by the quotient of friction to inertial forces, and indicating the transition of laminar to turbulent flow—usually lies between 1 and 10 for typical flow velocities of a few mm s^{-1} in micrometer-sized channels. This is far below the value of $\sim$2000 where turbulences and consequently, turbulence-induced mixing, can be expected. Without an elaborate additional instrumentation *e.g.* modification of the channel walls[8] that supports fast mixing, or electro-kinetic turbulent mixing modules,[9] the starting of reactions is solely based on molecular diffusion within the sample.

The time that a molecule needs to travel an average distance by diffusion is proportional to the square of the distance. Thus, diffusion-limited mixing can be sped up by miniaturization of the diffusion zone. A straightforward way to achieve this was introduced by Knight *et al.*[10] Here, a fast sheath flow of reactant A from two side channels merges with the flow in a middle channel containing another reactant B, thereby focussing the solution in this central zone down to a thin layer (see also the schematic drawing in Fig. 1, right inset). The control parameter in these mixing devices is the ratio of flow rates in the side and main channels. The characteristic mixing time for this so-called hydrodynamic focussing depends on the size of the flow layers as well as on the molecular diffusion coefficients of the sample.

After initiating the reaction by mixing, a crucial requirement to investigate fast reaction dynamics is a high spatial resolution of the readout process along the channel. In addition, proper readout parameters have to be defined which reliably reflect the reaction progress, and which can be determined with high sensitivity to avoid delays due to signal accumulation. Furthermore, to precisely translate the spatial position of the observation points along the channel to the exact time points of the reaction, the control and knowledge of the flow velocity is indispensable.

DOI: 10.1039/b406899h

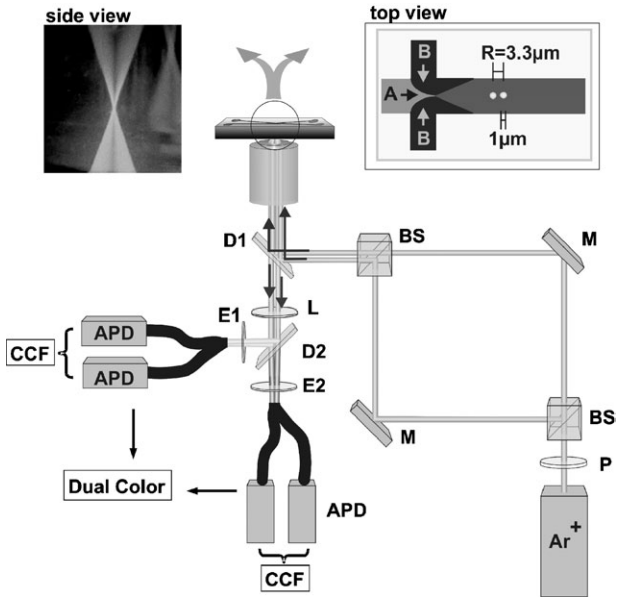

Fig. 1 Optical setup: Two parallel beams are coupled into the inverted microscope and focused by the objective, creating two excitation spots as illustrated in the left inset (image taken with a 20× objective). The microfluidic channel containing the reactants (here "A" and "B") is positioned onto the microscope objective and aligned in the direction of the laser spots (each spot has a diameter of 1 µm, while the distance R of the centres is 3.3 µm, right inset). The collected fluorescence from the sample is spectrally split and registered by four individual detectors. The cross correlation function (CCF) can be measured from the signals emitted from different spots, dual-color analysis is performed for signals of a detector pair that correspond to the same excitation spot (Ar^+: Argon ion laser, P: $\lambda/2$ wave plate, BS: beam splitter, M: mirror, L: focussing lens, D: dichroic mirrors (D1: Q565LP, D2: Q625LP), E: emission filters (E1: 585DF45, E2: 675DF45 + HQ655LP).

In this study, hybrid silicon elastomer/glass chips comprising a miniaturized channel system were employed as continuous flow reactors, adapted to a confocal setup for high-resolution optical detection.[11] Both the characteristic properties of the flow system as well as the progress of the reaction, could be simultaneously determined by means of fluorescence spectroscopy with high sensitivity and at low sample concentrations.

To precisely control the flow velocity within the sample, spatial fluorescence cross-correlation spectroscopy[12,13] was employed. This special mode of confocal analysis is performed by creating two slightly displaced laser foci by a single microscope objective. Each of these fluorescence excitation volumes is observed independently by a sensitive detector. By proper alignment of the sample flow inside the microfluidic channels, the emission signal from fluorescent molecules that are successively passing both excitation volumes is measured. Cross-correlation analysis of the signals results in a curve with a distinct maximum, corresponding to the average time that a molecule needs to travel the distance between both excitation volumes. Contrary to alternative imaging techniques, dual-beam cross-correlation in a confocal setup allows for very sensitive analysis, and for real-time monitoring of the flow velocity with high spatial resolution.

This optical setup was modified to observe the progress of the cleavage reaction of a double stranded DNA oligomer by the enzyme exonuclease III *via* dual-color fluorescence analysis. The complementary DNA strands are labelled with orange fluorescent TAMRA and red fluorescent Cy 5 dye molecules, respectively, promoting an efficient fluorescent resonant energy transfer (FRET) from the donor TAMRA to the acceptor Cy 5 if both strands are annealed and intact. The dual-color fluorescence analysis of the DNA was supported by spectral discrimination of the emission signal in two detection channels, quantifying donor and acceptor emission. During reaction, the enzyme cuts the nucleotides beginning at the 3′ end.[14] The spatial separation of the dyes results in the loss of energy transfer. Thus, the decrease of fluorescence intensity in the acceptor detection channel purified of cross-talk from the donor detection channel reports directly the progress of the cleavage reaction.

Although standard dual-color cross-correlation in principle allows the direct determination of slow irreversible enzymatic cleavage reactions[15] with reaction rates of a few minutes (*i.e.* reactions that are clearly slower than the time needed for data acquisition), fast reaction mechanisms could so far not be resolved. The introduction of µCF could thus greatly improve the time resolution whithout a significant reduction of detection sensitivity.

Experimental section

The optical setup based on a dual-beam setup[12,13] is modified (Fig. 1). The 514 nm line of an Ar-Ion laser (Lasos, Jena, Germany) passes two polarizing beam splitter cubes to create two parallel but slightly displaced laser beams. For equalizing the intensity of both laser beams, a $\lambda/2$-waveplate is used. The beams are coupled into an inverted microscope (Olympus IX 50) and focussed by an objective (Olympus UplanApo 60×, NA1.2) creating two excitation spots ($I = 80$ kW cm^{-2}). The fluorescence from each spot is spectrally split by a dichroic mirror (specifications in figure caption, all purchased from AHF, Tübingen, Germany), passes respective band pass filters and is then imaged onto the entrance slits of two fiber bundles serving as confocal pinholes. The bundles consist of two separate fibers with distinct aperture distances (200 µm) corresponding to the distance of the focused laser spots. With the objective of 60× magnification, the centres of both laser spots have a distance of 3.3 µm. Each fiber is connected to separate detectors (SPCM CD3017, EG&G). In this way, four detection channels are created, allowing both the determination of *flow velocities* by spatial cross-correlation of signals from the same fiber bundle, and the dual-color fluorescence analysis from the spectrally distinct signals measured by different fiber bundles at the same spatial position. The data acquisition is performed using two correlator cards (ALV Langen, Germany). For calculations and data fitting procedures, Origin software (Microcal) was employed. The optical setup was calibrated by standard autocorrelation analysis of the four detection channels with a tetramethylrhodamine solution (under diffusion condition, *i.e.* without flow). In the case of optimal adjustment, the four autocorrelation curves match perfectly, indicating the same size of the spectrally and spatially distinct measurement volumes. From the autocorrelation function, the dimensions of the approximately cylindrical detection volume could be determined.[16] It has a radius of 0.5 µm and a half length of 2.85 µm (data not shown).

Spectra were taken with a fiber optic spectrometer (S2000, Ocean Optics).

The microstructured channels are formed in poly(dimethyl)-siloxane (PDMS, Sylgard 184, Dow Corning) using a teflon coated silicon wafer as mould (fabricated by GeSim, Großerkmannsdorf, Germany) and cut to a size of $\sim 2 \times 3$ cm. They are sealed by a coverslip tightly adhering to the silicone rubber. The sample supply is facilitated by punched holes. The channels are 15 µm high and 25 µm width (narrow section: 6 µm). The total length of the observation channel is 10 mm. The channels are fabricated freshly before each experiment to minimize contamination by dust. To generally prevent adsorption of protein to the channel walls, a buffer solution containing BSA (1 µg ml^{-1}) is introduced and incubated for 30 min. To apply flow velocities faster than 2 mm s^{-1}, the coverslip and the PDMS structure are treated in a plasma cleaner for 5 min and immediately pressed together, so that they form a strong

bond. The holes at the end of the channels are connected to syringe pumps by tubes.

For the continuous flow reaction, double stranded DNA (28 bp) is labelled with Cy5 (Amersham) at the 5′ end of one single strand and carboxytetramethylrhodamine (TAMRA, Molecular Probes) at position 14 of the complementary strand. 10–30 μl of DNA solution (3.7 nM in 1× NE buffer 1 pH 7, New England Biolabs) is fed into the input reservoir of the middle channel, the side channel reservoirs were filled with the same amount of an exonuclease III solution (New England Biolabs, 15–793 μM in the same buffer solution). All experiments are carried out at 21 °C.

Results and discussion

Mixing in a microchannel

Mixing is facilitated using a crossed microfluidic channel system, where the DNA substrate is fed into the middle channel and enzyme solution into the side channels. At the intersection, the solutions merge to three parallel fluid layers. The thickness of each layer is determined by the flow rates that can be regulated by the hydrodynamic pressures exerted by different heights of the respective liquid reservoirs. For the here described experiments, the flow rates at each entrance channel are identical, which are precisely controlled by measuring the flow velocities *via* dual-beam cross-correlation (see below).

The efficient mixing of two different solutions inside the channels is illustrated in Fig. 2. The intensity profiles of TAMRA fluorescence perpendicular to the flow direction indicate that the mixing of the DNA solution is started directly at the channel junction. However, to circumvent artifacts arising from non-uniform concentration profiles, a narrowing neck section was introduced in the main channel shortly after the channel junction, resulting in a supplementary narrowing of the parallel flow layers. A complete mixing of both solutions, *i.e.* an evenly distributed fluorescence intensity, is obtained immediately after passing this neck and thus, the reaction conditions are equalized over the channel cross-section. Considering the measured flow velocities of the solutions, the mixing time can be determined. For the here described experiments with typical velocities of max. 1.3 mm s^{-1}, it is approximately 100 ms.

By adaptation of self-made tubing connectors and syringe pumps, flow velocities up to ~50 mm s^{-1} are accessible. However, for fast flow rates, the concentration profile of sample due to incomplete mixing has to be taken into account. In this context, a further decrease of the channel dimensions that supports faster mixing would be useful.

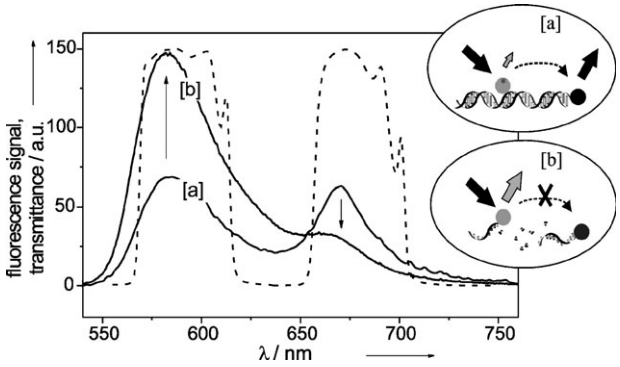

Fig. 3 Spectra of the DNA oligomer labelled with carboxy-tetramethylrhodamine (TAMRA) and Cy5 before (a) and after (b) the enzymatic cleavage reaction. The dotted lines show the transmission of the used emission filters to detect TAMRA and Cy5 fluorescence.

DNA cleavage reaction

We were carrying out the cleavage reaction of a double stranded DNA oligomer (28 bp) by the enzyme exonuclease III that cuts the nucleotides beginning at the 3′ end. The part strands of the DNA oligomer are labelled with carboxytetramethylrhodamine (TAMRA) and Cy 5, respectively. The spectra of the DNA before and after the enzymatic cleavage reaction of the nucleotides are shown in Fig. 3.

Assuming a reaction scheme without fluorescent intermediates, the intensity of the Cy 5 fluorescence (I_{Cy5}) can be calculated in the following way:[17]

$$I_{Cy5} = \eta_{intact}[DNA]_{intact} + \eta_{cleaved}[DNA]_{cleaved} \qquad (1)$$

where $[DNA]_{intact}$ and $[DNA]_{cleaved}$ are the concentration of DNA, and η_{intact} an $\eta_{cleaved}$ are the molecular brightnesses of Cy 5 in the presence and absence of energy transfer, *i.e.* if Cy 5 is bound to the intact or cleaved DNA strand, respectively. The brightness of Cy 5 in the intact DNA (η_{intact}) has a constant value, depending on the energy transfer efficiency from TAMRA to Cy5. After the reaction, $\eta_{cleaved} = 0$ can be assumed and thus, the concentration of intact DNA is directly proportional to the intensity of Cy 5 fluorescence. Since the applied laser intensity is low, we neglect photobleaching that is generally very weak in flowing systems.

For fast and sensitive measurements in the microfluidic channel system, we determined the fluorescence intensity, *i.e.* the count rate of detected photons, by spectral filtering in two detection channels (I_{red} and I_{orange}), corresponding to donor and acceptor fluorescence.

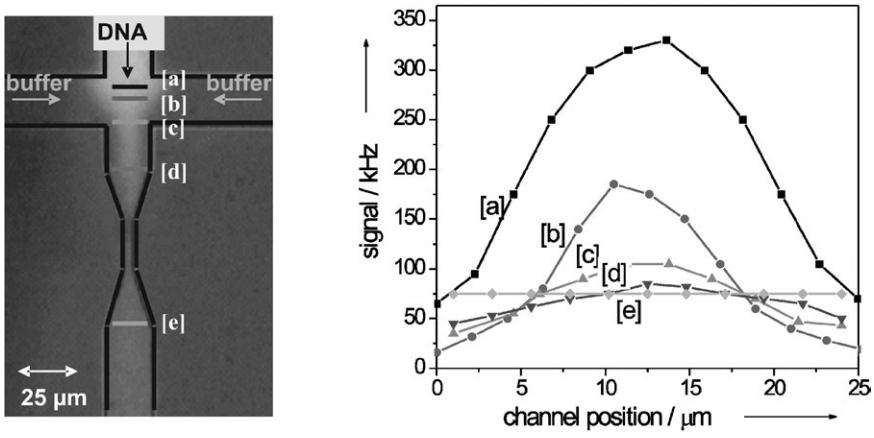

Fig. 2 Mixing of the two reactants is performed using a crossed microchannel. To verify appropiate mixing, we determined the distribution of the stained DNA after mixing with buffer solution, by measuring the fluorescence intensity perpendicular to the flow direction at different channel positions (a–e). Complete mixing would be indicated by a constant intensity profile corresponding to a uniform distribution of DNA. We could observe this after the narrow section of the channel. Thus, at this position the first observation point is marked.

For calculation of the "pure" Cy 5 fluorescence intensity (I_{cy5}) from the experimentally determined signal in the red detection channel it has to be considered that the count rate does not decrease to zero even in the case of completely cleaved DNA. After subtraction of the background mainly due to stray light from the microchannel and the constant direct excitation of Cy 5 at $\lambda = 514$ nm (summarized in $I_{red,bg}$), the remaining signal is caused by cross talk, *i.e.* the red fluorescence tail from TAMRA. It is determined to be 8.3% of the signal intensity of TAMRA (I_{TAMRA}). Thus I_{Cy5} is calculated as follows:

$$I_{Cy5} = I_{red} - I_{red,bg} - 0.083 \times I_{TAMRA} \quad (2a)$$

I_{TAMRA} is the signal in the orange detection channel (I_{orange}) minus a constant background ($I_{red,bg}$):

$$I_{TAMRA} = I_{orange} - I_{orange,bg} \quad (2b)$$

I_{Cy5} is normalized by dividing the values by the initial fluorescence intensity ($I_{Cy5,0}$), eliminating variations due to experimental (*i.e.* pipetting) errors.

For the applied laser intensity and the DNA concentration of 3.7 nM, the initial signals of the DNA solution are typically $I_{orange} = 250$ kHz and $I_{red} = 350$ kHz. The average background signals were determined for pure buffer solution filled into the microfluidic channels, $I_{orange,bg} = 8.4$ kHz and $I_{red,bg} = 3.4$ kHz. The red signal due to direct excitation of Cy 5 by $\lambda = 514$ nm is 50 kHz.

After initiating the cleavage reaction inside the microchannel by mixing, the decrease of I_{Cy5} is followed at 15 different positions (p) between 0–6000 μm downstream (Fig. 4, top).

A monoexponential decrease of the fluorescence intensity can be observed, in full agreement with the proposed reaction mechanism that a fast steady state formation of the DNA–enzyme complex is followed by a first-order cleavage reaction with the reaction rate $k_{reaction}$ (The index "0" indicates the values at position 0):

$$\frac{I_{Cy5}}{I_{Cy5,0}} = \frac{[DNA]_{intact}}{[DNA]_0} = \exp(-k_{reaction}p) \quad (3)$$

At high flow rates, the reaction is delayed and deviations from non-exponential behavior are apparent, reflecting the time needed until the complete DNA cleavage can first be detected, as well as non-idealities in mixing. To rule out unspecific removal of educt or product due to adsorption to the channel walls, the microfluidic channels were incubated with BSA buffer. The intensities of orange and red fluorescence (*i.e.*, the concentrations) were checked for a pure intact DNA substrate, as well as for free nucleotides labelled with the respective fluorophores. They proved to be constant all along the observed channel length.

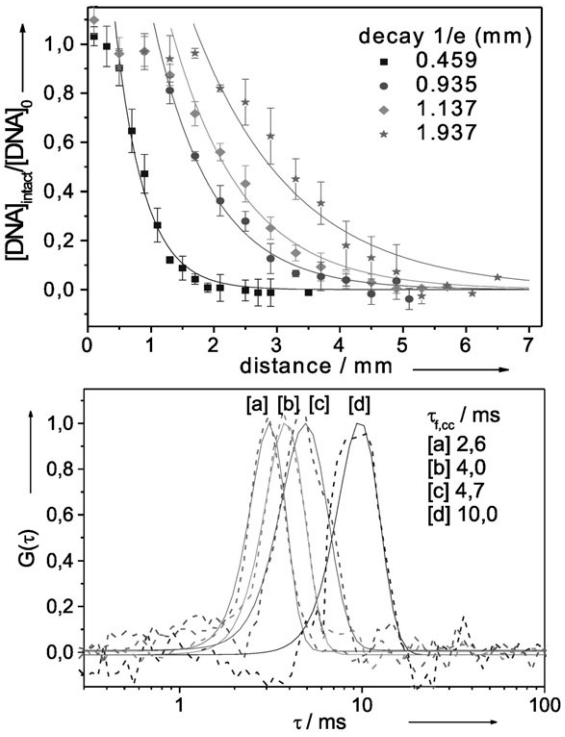

Fig. 4 The reaction is followed by determination of the fluorescence intensity of the acceptor dye, Cy 5 (divided by the initial value) that is directly related to the concentration of the uncleaved DNA (top, with single exponential fit, eqn. (3)). Simultaneously, the flow velocities are determined *via* cross-correlation analysis allowing the transformation of the spatial dimension into the temporal information (bottom, dotted lines: original data, solid lines: fit curves, using eqn. (4)).

Flow measurements

To determine the exact flow time from the mixing point to the observation point, representing the reaction time, spatial fluorescence cross-correlation spectroscopy is employed.

Here, the flow velocity v is analyzed by cross-correlation of the signals emitted from the two displaced focal spots. By subtraction of the resulting forward and backward cross-correlation curves for the time τ, the "true" directional cross-correlation signal $G(\tau)$ exhibits a maximum for the flow time $\tau_{f,cc}$. The flow time correspond to the time that the fluorescent molecules need to travel from the center of the first to the second focal spot, if the flow direction is aligned with the connecting axis of the two foci ($\alpha = 0$). The flow time $\tau_{f,cc}$ is determined using the following expression:[12]

$$G_{cc}(\tau) = \left[N\left(1+\frac{\tau}{\tau_d}\right)\sqrt{1+\frac{\omega_0^2\tau}{z_0^2\tau_d}}\right]^{-1} \exp\left[-\frac{R^2}{\omega_0^2}\frac{1}{(1+(\tau/\tau_d))} \times\left(\frac{\tau^2}{\tau_{f,cc}^2}+1-2\frac{\tau}{\tau_{f,cc}}\cos\alpha\right)\right] \quad (4)$$

with N, the number of particles flowing through *both* focused spots, and τ_d, the average transit time of the molecules through one focal element in the case of pure diffusion. ω_0 and z_0 are the $1/e^2$ dimensions of the detection volumes in the radial and axial direction. R is the distance of the focal spots (here: 3.3 μm, see experimental section).

Hence, the position of the observation point p is translated into the reaction time t as follows:

$$t = \frac{p}{v} = \frac{p\tau_{f,cc}}{R} \quad (5)$$

The flow velocity v determined in the center of the channel after mixing of the reactants is varied from 0.3 to 1.3 mm s^{-1} (flow times between 2.6 and 10.0 ms, Fig. 3).

Translating position into time for the results in Fig. 4 (bottom), we determine the reaction rate of the cleavage reaction with $k_{reaction} = (0.75 \pm 0.04)$ s^{-1}. It is nicely confirmed for all applied flow velocities.

Under saturation conditions, the rate of digestion is about 10 nucleotides per second, since the enzyme has to cut 14 nucleotides (nt) until the energy transfer is eliminated which is in the range of the reaction rates previously measured by Hoheisel[18] ($\sim$1–16 nt s^{-1}). However, differences in temperature and buffer composition might influence the reaction rates, as well as the low melting temperature of the short DNA double strands, resulting in early strand separation and after cutting just a few (instead of 14) nucleotides.

Finally, the reaction is followed for various enzyme concentrations between 15 and 40 μmol l^{-1} at constant flow velocity of 0.3 mm s^{-1}.

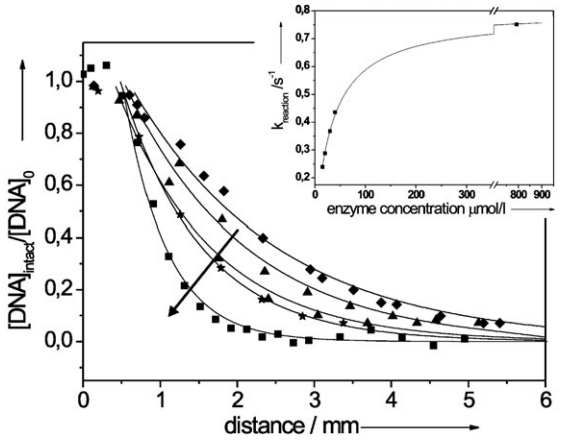

Fig. 5 DNA cleavage reaction for varying enzyme concentrations (15, 20, 30, 40 and 793 μmol l^{-1}). For increasing enzyme concentration (indicated by the arrow), the reaction proceeds faster, until saturation is reached (inset). The determined spatial reaction rates (in 1 mm^{-1}) are translated into the temporal reaction rates (1 s^{-1}, inset) using eqn. (5). The applied flow velocity was 0.3 mm s^{-1} in all experiments.

We were applying the same analysis as described above. The reaction rates obtained (Fig. 5) are—as expected—increasing with increasing enzyme concentration (approximately linear for low concentrations). For high enzyme concentration a saturation value of the reaction rate is reached in good agreement with the theoretically expected course (see also ref. 18).

Conclusion

In this study, a new scheme for the investigation of fast reactions based on confocal fluorescence spectroscopy in a miniaturized continuous flow (μCF) reactor was presented. By dual-beam cross-correlation, the flow velocity inside the microchannel can be comfortably controlled. Simultaneously, the reaction progress was followed by dual-color analysis, and the reaction rate of the DNA cleavage could be determined. To overcome the drawbacks of conventional CF reactors with regard to high sample consumption, self-made microfluidic chips were employed, allowing an economical expenditure of sample solution of a only few μL, while low concentrations (nM) could be used due to the high sensitivity of the detection setup. The overall sample consumption thus amounted to only $\sim 10^{-14}$ mol = 10 fmol which makes the device extremely valuable for studying (biochemical) reactions where the amount of available sample is often very low. A broad temporal range from μs to seconds is accessible, although for fast velocities above 1 mm s^{-1} the non-uniform concentration profile needs to taken in to account.

Due to the sensitivity of the optical setup that supports the detection of single molecules, the concept can be extended to the study individual molecular events, where subpopulations can be resolved and more detailed information of the reaction mechanism be obtained.[19,20]

References

1 M. Eigen, *Angew. Chem.*, 1968, **21**, 892–906.
2 B. Nölting, R. Golbik and A. R. Fersht, *Proc. Natl. Acad. Sci. USA*, 1995, **92**, 10668–10672.
3 C. M. Jones, E. R. Henry, Y. Hu, C. K. Chan, S. D. Luck, A. Bhuyan, H. Roder, J. Hofrichter and W. A. Eaton, *Proc. Natl. Acad. Sci. USA*, 1993, **90**, 11860–11864.
4 H. Hartridge and F. J. W. Roughton, *Proc. R. Soc. London, Ser. A*, 1923, **104**, 376–394.
5 M. C. R. Shastry, S. D. Luck and H. Roder, *Biophys. J.*, 1998, **74**, 2714–2721.
6 S. A. Pabit and S. J. Hagen, *Biophys. J.*, 2002, **83**, 2872–2878.
7 M. Kakuta, F. G. Bessoth and A. Manz, *Chem. Rec.*, 2001, **1**, 395–405.
8 A. D. Stroock, S. K. W. Dertinger, A. Ajdari, I. Mezit, H. A. Stone and G. M. Whitesides, *Science*, 2002, **295**, 647–651.
9 M. H. Oddy, J. G. Santiago and J. C. Mikkelson, *Anal. Chem.*, 2001, **73**, 5822–5832.
10 J. B. Knight, A. Vishwanath, J. P. Brody and R. H. Austin, *Phys. Rev. Lett.*, 1998, **80**, 3863–3866.
11 P. S. Dittrich and P. Schwille, *Anal. Chem.*, 2003, **75**, 5767–5774.
12 M. Brinkmeyer, K. Dörre, J. Stephan and M. Eigen, *Anal. Chem.*, 1999, **71**, 609–616.
13 P. S. Dittrich and P. Schwille, *Anal. Chem.*, 2002, **74**, 4472–4479.
14 B. Weiss, in *The enzymes*, Academic Press, New York, 1981, vol. 14, pp. 203–231.
15 P. Schwille, J. Bieschke and F. Oehlenschläger, *Biophys. Chem.*, 1997, **66**, 211–228.
16 R. Rigler, Ü. Mets, J. Widengren and P. Kask, *Eur. Biophys. J.*, 1993, **22**, 169–175.
17 P. Schwille, F.-J. Meyer-Almes and R. Rigler, *Biophys. J.*, 1997, **72**, 1878–1886.
18 J. D. Hoheisel, *Anal. Biochem.*, 1993, **209**, 238–246.
19 T. Ha, A. Y. Ting, J. Liang, W. B. Caldwell, A. A. Deniz, D. S. Chemly, P. G. Schulz and S. Weiss, *Proc. Natl. Acad. Sci. USA*, 1999, **96**, 893–898.
20 E. A. Lipman, B. Schuler, O. Bakajin and W. A. Eaton, *Science*, 2003, **301**, 1233–1235.